

from an unknown N_γ contribution on the right,

$$\Sigma^{(1)} \cong f_s^{(1)} \quad (\text{A1})$$

and

$$\Sigma^{(2)} \cong \gamma_{N_\alpha}^{(2)} + N + f_s^{(2)}. \quad (\text{A2})$$

The nucleon trajectory makes no contribution to $\Sigma^{(1)}(N, M^2)$ because on the spin shell the nucleon pole does not appear in $A^{(1)}$. We see from Fig. 2 that $\Sigma^{(1)}$ is indeed roughly constant with N . From (2.1) or (2.3) and (2.6) and the definition of the πNN coupling constant, one finds that

$$\begin{aligned} \gamma_{N_\alpha}^{(2)}(M^2) &= \frac{3}{2} \frac{g_{\pi NN}^2}{4\pi} \frac{d\alpha_{N_\alpha}}{du} \Big|_{M^2} \\ &= 22/\text{GeV}^2, \end{aligned} \quad (\text{A3})$$

using the Chew-Frautschi trajectory $\alpha_{N_\alpha} = -0.39$

+1.0 u .²³ Amusingly, a straight-line fit by eye to the curve of $\Sigma^{(2)}$ yields a slope of 20/GeV². Thus the N -dependence of the $\Sigma^{(2)}$ at $u=M^2$ is qualitatively right, but compared with those at $u=-0.13$ GeV², the wiggles around the extrapolated high-energy behavior are now moderately large.

Figure 3 depicts the $\Sigma^{(2)}(N, u)$, evaluated once more in terms of resonances, at $u=M_{33}^2$, the mass squared of the 33 resonance. The wiggly pattern of $u=M^2$ is repeated.³⁹ We see that the duality at $u=-0.13$ GeV², where the extrapolated high-energy imaginary part (zero) is extremely well conformed to by the resonances down to surprisingly low energy, is a very special behavior not duplicated at general u .

³⁹ For $u=M_{33}^2$, we have estimated the Regge part of the right-hand side of (2.14) from the results of Ref. 5. We find no conclusive evidence for a strong fixed pole at this u .

Parity-Violating Internucleon Potential in Nuclear Reactions of the n - p System*

E. HADJIMICHAEL

Department of Physics, State University of New York at Stony Brook, Stony Brook, New York 11790

and

Department of Physics, Fairfield University,† Fairfield, Connecticut 06430

AND

EPHRAIM FISCHBACH

Institute for Theoretical Physics, State University of New York at Stony Brook, Stony Brook, New York 11790

and

Department of Physics, Purdue University, Lafayette, Indiana 47907‡

(Received 30 September 1970)

The parity-violating nucleon-nucleon interaction arising from weak one-pion exchange and one-vector-meson exchange, has been added to the strong, semiphenomenological nucleon-nucleon interaction and its effects on the n - p system studied in detail. The parity admixtures in the initial and final states of the n - p system in deuteron photodisintegration and in radiative n - p capture have been calculated for various models of the weak-interaction Hamiltonian H_w and found to be in the range 10^{-9} - 10^{-7} depending on the model of H_w , thus allowing for the possibility of discriminating among models of H_w by comparison to experiment.

I. INTRODUCTION

A VARIETY of models of the weak-interaction Hamiltonian H_w have been proposed recently to account for a number of features of the weak interactions, such as the $|\Delta I| = \frac{1}{2}$ rule, CP violation, and divergences in higher-order processes.¹⁻⁶ All of these

models can be cast into an *effective* current-current form

$$\begin{aligned} H_w^{(a)}(x) &= \frac{G}{\sqrt{2}} g_{abc} [j_\mu^{(b)}(x) j_\mu^{(c)}(x) + \text{H.c.}], \\ G &\cong 10^{-5}/m_N^2, \end{aligned} \quad (1)$$

where a , b , and c are $SU(2)$ or $SU(3)$ indices, and g_{abc} a set of constants depending on the particular model of H_w . These models can be distinguished from one another by their predictions for weak strangeness-

* Work supported by AEC Contract Nos. 31-6028B and AT(30-1)-3668B.

† Permanent address.

‡ Permanent address.

¹ R. F. Dashen, S. C. Frautschi, M. Gell-Mann, and Y. Hara, in *The Eightfold Way*, edited by M. Gell-Mann and Y. Ne'eman, (Benjamin, New York, 1964), p. 254.

² F. C. Michel, Phys. Rev. **133**, B329 (1964), and additional references therein.

³ E. Fischbach, Phys. Rev. **170**, 1398 (1968), and references therein.

⁴ E. Fischbach and K. Trabert, Phys. Rev. **174**, 1843 (1968).

⁵ D. Tadić, Phys. Rev. **174**, 1694 (1968).

⁶ E. Fischbach, D. Tadić, and K. Trabert, Phys. Rev. **186**, 1688 (1969); E. Fischbach, D. Tadić, and K. Trabert, in *High Energy Physics and Nuclear Structure*, edited by S. Devons (Plenum, New York, 1970), p. 742.

conserving processes, such as parity-violating nucleon-nucleon scattering arising from weak one-pion exchange and one-vector-meson exchange. This parity-violating meson exchange gives rise to a parity-violating contribution V_{12}^{pv} to the total nucleon-nucleon potential V_{12} . In turn, V_{12}^{pv} is responsible for a variety of parity-violating processes in nuclear physics such as irregular α widths in nuclear α decay,^{2,7,8} circular polarization of photons and asymmetries in the angular distribution of photons in nuclear electromagnetic transitions,^{2,9} and a number of asymmetries in few-nucleon reactions, such as deuteron photodisintegration, radiative n - p capture, and radiative neutron-deuteron capture.^{5,10-13} There is a special advantage in working with few-nucleon reactions, namely, that the nuclear wave functions can be obtained quite accurately, whereas those of heavy nuclei are less well known.

In this paper we report results of calculations of the effects of parity admixture in the initial and final states of the n - p system undergoing the two reactions $d(\gamma, n)p$ and $p(n, \gamma)d$. The quantities calculated are, in the case of deuteron photodisintegration, (a) an asymmetry δ in the cross section of the emergent proton about the plane of polarization of linearly polarized incident photons, and (b) the components of polarization P_z' and P_x' of the emergent nucleons in directions defined by \mathbf{k} and $(\boldsymbol{\kappa} \times \mathbf{k}) \times \mathbf{k}$, for unpolarized incident photons, where \mathbf{k} and $\boldsymbol{\kappa}$ are the wave vectors for outgoing nucleons and incident photons, respectively. $\boldsymbol{\kappa}$ defines the positive z axis of an orthogonal system and \mathbf{k} defines the z' axis of a second orthogonal system which is obtained from the first by two Euler rotations through angles ϕ about the z axis and θ about the y' axis. In the case of n - p radiative capture, the degree of circular polarization P_γ of emergent photons is a manifestation of parity violation.

We define

$$\delta = \frac{d\sigma(\theta, \phi) - d\sigma(\theta, -\phi)}{d\sigma(\theta, \phi) + d\sigma(\theta, -\phi)}, \quad (2)$$

where $d\sigma(\theta, \phi)$ is the differential cross section for outgoing protons, and

$$P_\gamma = \frac{d\sigma^-(\theta, \phi) - d\sigma^+(\theta, \phi)}{d\sigma^-(\theta, \phi) + d\sigma^+(\theta, \phi)}, \quad (3)$$

where $d\sigma^-(\theta, \phi)$ and $d\sigma^+(\theta, \phi)$ are the cross sections for outgoing photons from n - p radiative capture, left-circularly polarized and right-circularly polarized, respectively. P_x' and P_z' and $d\sigma(\theta, \phi)$ are defined in terms of reaction amplitudes S_{mi} as in Rustgi *et al.*¹⁴ $d\sigma^-(\theta, \phi)$ and $d\sigma^+(\theta, \phi)$ are obtained from the amplitudes S_{mi} for photodisintegration by employing invariance under time reversal.

II. NUCLEAR FORCE, DEUTERON, AND n - p SCATTERING AMPLITUDES

The parity-violating potentials investigated are those described in Refs. 3 and 4. In general,

$$V_{12}^{\text{pv}} = V_{12}^\pi + V_{12}^V,$$

where the weak pion-exchange potential V_{12}^π is

$$V_{12}^\pi = A \left\{ \Gamma(\boldsymbol{\sigma}_1 + \boldsymbol{\sigma}_2) \cdot \left[\mathbf{p}_{12}, \frac{e^{-\mu_\pi r}}{r} \right]_- T_{12}^{(-)} \right\},$$

$$T_{12}^{(\pm)} = \tau_1^{(+)} \tau_2^{(-)} \pm \tau_1^{(-)} \tau_2^{(+)}. \quad (4)$$

The symbols $[\]_-$ and $[\]_+$ denote commutation and anticommutation, respectively.

The weak vector-meson-exchange potential V_{12}^V is

$$V_{12}^V = \left(-\frac{\hbar_A f_\rho}{8\pi\sqrt{2}m_N} \right) \left\{ i(\boldsymbol{\sigma}_1 \times \boldsymbol{\sigma}_2) \cdot \left[\mathbf{p}_{12}, \frac{e^{-\mu_\rho r}}{r} \right]_- \times (1 + \mu_p - \mu_n) \right. \\ \times [(\tau_1^{(+)} \tau_2^{(-)} + \tau_1^{(-)} \tau_2^{(+)}) + \frac{1}{4} B \tau_1^{(z)} \tau_2^{(z)} + \frac{1}{4} C \xi (\tau_1^{(z)} + \tau_2^{(z)})] + i(\boldsymbol{\sigma}_1 \times \boldsymbol{\sigma}_2) \cdot \left[\mathbf{p}_{12}, \frac{e^{-\mu_\rho r}}{r} \right]_- \\ \times (\frac{1}{3}\sqrt{3}C'(1 + \mu_p + \mu_n) \times (\tau_1^{(z)} + \tau_2^{(z)}) + \frac{1}{2}\sqrt{3}D\xi) + (\boldsymbol{\sigma}_1 - \boldsymbol{\sigma}_2) \cdot \left[\mathbf{p}_{12}, \frac{e^{-\mu_\rho r}}{r} \right]_+ \\ \times [(\tau_1^{(+)} \tau_2^{(-)} + \tau_1^{(-)} \tau_2^{(+)}) + \frac{1}{4} B \tau_1^{(z)} \tau_2^{(z)}] + (\boldsymbol{\sigma}_1 - \boldsymbol{\sigma}_2) \cdot \left[\mathbf{p}_{12}, \frac{e^{-\mu_\rho r}}{r} \right]_+ (\frac{1}{2}\sqrt{3}D\xi) + (\boldsymbol{\sigma}_1 \tau_1^{(z)} - \boldsymbol{\sigma}_2 \tau_2^{(z)}) \cdot \left[\mathbf{p}_{12}, \frac{e^{-\mu_\rho r}}{r} \right]_+ \\ \left. \times (\frac{1}{4}\sqrt{3}C') + (\boldsymbol{\sigma}_1 \tau_2^{(z)} - \boldsymbol{\sigma}_2 \tau_1^{(z)}) \cdot \left[\mathbf{p}_{12}, \frac{e^{-\mu_\rho r}}{r} \right]_+ \times (\frac{1}{2}C\xi) \right\},$$

⁷ D. H. Wilkinson, Phys. Rev. **109**, 1603 (1958).

⁸ M. Gari and H. Kummel, Phys. Rev. Letters **23**, 26 (1969); E. M. Henley, T. Keliher, and D. U. L. Yu, *ibid.* **23**, 941 (1969); M. Gari, Phys. Letters **31B**, 627 (1970).

⁹ R. J. Blin-Stoyle, Phys. Rev. **120**, 181 (1960); R. Boehm and E. Kankeleit, Nucl. Phys. **A109**, 457 (1968); B. H. J. McKellar, Phys. Rev. Letters **20**, 1542 (1968).

¹⁰ R. J. Blin-Stoyle and H. Feshbach, Nucl. Phys. **27**, 395 (1961).

¹¹ G. S. Danilov, Phys. Letters **18**, 40 (1965).

¹² O. D. Dal'karov, Zh. Eksperim. i Teor. Fiz. Pis'ma v Redaktsiyu **2**, 310 (1965) [Soviet Phys. JETP Letters **2**, 197 (1965)].

¹³ F. Partovi, Ann. Phys. (N. Y.) **27**, 114 (1964).

¹⁴ M. L. Rustgi, W. Zernik, G. Breit, and D. J. Andrews, Phys. Rev. **120**, 188 (1960).

$$\Gamma = (1.25 \times 10^5 \text{ sec}^{-1/2}) \times \frac{g_{\pi NN} \mu_\pi}{8\pi\sqrt{2}m_N}, \quad \mu_\pi = m_\pi c/\hbar, \quad g_{\pi NN} = 13.5, \quad h_A f_\rho = m_\rho^2 G G_A \cos^2\theta,$$

$$G G_A = 1.23 \times 10^{-5}/m_N^2 \quad \text{and} \quad \frac{2\hbar h_A f_\rho \mu_\pi^2}{8\pi\sqrt{2}m_N} = 0.9534 \times 10^{-5} \text{ MeV}, \quad 2\Gamma\hbar\mu_\pi^2 = 0.428 \times 10^{-5} \text{ MeV}. \quad (5)$$

m_N , m_π , and m_ρ are the nucleon, pion, and ρ -meson masses, respectively. The values of the five parameters A , B , C , C' , and D for the various models under consideration are listed in Table I.¹⁵

V_{12}^V can be split into two parts, namely, $V_{12}^V = V_{\text{I}}^V + V_{\text{II}}^V$ with

$$V_{\text{I}}^V = -i \left(\frac{2\hbar h_A f_\rho}{8\pi\sqrt{2}m_N} \right) \left\{ \left[\mu f_{R^{\text{I}}} \left(\frac{\mathbf{S}^- \cdot \mathbf{r}}{r} \right) P_\sigma - \mathbf{S}^- \cdot [\nabla_{\mathbf{r}}, f_{R^{\text{I}}}]_+ \right] \times (T^{(+)} + \frac{1}{4} B \tau_1^{(z)} \tau_2^{(z)}) \right. \\ \left. + \left[f_{R^{\text{I}}} \left(\frac{\mathbf{S}^- \cdot \mathbf{r}}{r} \right) \times P_\sigma - \mathbf{S}^- \cdot [\nabla_{\mathbf{r}}, f_{R^{\text{I}}}]_+ \right] \left(\frac{1}{2} \sqrt{3} D \xi \right) \right\} \quad (6)$$

and

$$V_{\text{II}}^V = i \frac{2\hbar h_A f_\rho}{8\pi\sqrt{2}m_N} \left\{ \frac{1}{4} \sqrt{3} C' (\sigma_1 \tau_1^{(z)} - \sigma_2 \tau_2^{(z)}) \cdot [\nabla_{\mathbf{r}}, f_{R^{\text{II}}}]_+ + \frac{1}{2} C \xi (\sigma_1 \tau_2^{(z)} - \sigma_2 \tau_1^{(z)}) \cdot [\nabla_{\mathbf{r}}, f_{R^{\text{II}}}]_+ \right\}. \quad (7)$$

Here the commutator $[\]_-$ has been written out explicitly,

$$\sigma_1 \times \sigma_2 = i(\sigma_1 - \sigma_2) P_\sigma = i \mathbf{S}^- P_\sigma, \quad \mu = 1 + \mu_p - \mu_n,$$

$$f_{R^{\text{I}}} = \frac{d}{dr} \left(\frac{e^{-\mu_\rho r}}{r} \right), \quad f_{R^{\text{II}}} = e^{-\mu_\rho r}/r,$$

and P_σ is the spin exchange operator. V_{I}^V connects states of opposite parity and isospin difference $|\Delta \mathbf{I}| = 0, 2$. V_{12}^V and V_{II}^V connect states of opposite parity and isospin difference $|\Delta \mathbf{I}| = 1$.

The photon-deuteron interaction H_{em} employed is the one developed by Breit and Rustgi,¹⁶ conveniently expanded in terms of electromagnetic multipoles. We limit ourselves to $E1$ - $M1$ transitions, and hence only low energies will be considered where these transitions are the only important ones.

The deuteron, in the presence of the weak potential, Eqs. (4) and (5), as well as a strong potential, is a mixture of 3S_1 , 3D_1 , 3P_1 , and 1P_1 states. The n - p scattering wave function in the incoming mode has the general form

$$\psi_m^- = \frac{(4\pi)^{1/2}}{kr} \sum_{J,\lambda} \sum_{l,s;l',s'} i^l (2l+1)^{1/2} (l,0,s,m/J,m) e^{i\delta_\lambda} \\ \times U_{l,s,\lambda} U_{l',s',\lambda} v_{l',s',\lambda}^{J,s',\lambda}(r) Y_m^{l',s',J}(\theta,\phi), \quad (8)$$

where l , s (and l' , s') make up one index with values $(l=J-1, s=1)$, $(l=J+1, s=1)$, $(l=J, s=1)$, $(l=J, s=0)$. λ stands for α , β , γ , ϵ that denote the four "eigenstates," in the sense of Blatt and Biedenharn,¹⁷ of the S matrix for n - p scattering. In the presence of only strong interactions the α eigenstate is a mixture of $(l=J-1, s=1)$ and $(l=J+1, s=1)$ states, the β

eigenstate is also a mixture of $(l=J-1, s=1)$ and $(l=J+1, s=1)$ states, the γ eigenstate is the singlet $(l=J, s=0)$, and the ϵ eigenstate is the uncoupled triplet $(l=J, s=1)$. In the presence of strong and weak interactions, it is easy to show that, to first order in V_{12}^{pv} , these partial-wave states, which we shall call "strong," are not affected by V_{12}^{pv} . However, there are new partial-wave states, which we shall call "weak," entering into the picture so that now the α and β eigenstates of the 4×4 S matrix are a mixture of $(l=J-1, s=1)$, $(l=J+1, s=1)$, $(l=J, s=0)$, and $(l=J, s=1)$. The γ eigenstate is a mixture of $(l=J-1, s=1)$, $(l=J+1, s=1)$, $(l=J, s=0)$. Finally the ϵ eigenstate is a mixture of $(l=J-1, s=1)$, $(l=J+1, s=1)$, and $(l=J, s=1)$. $U_{l,s,\lambda}$ are the matrix elements of a 4×4 orthogonal matrix, that are functions of the coupling parameters that couple the various orbital momentum states allowed by the interaction, for any given total angular momentum. δ_λ^J are the phase shifts.

To first order in V_{12}^{pv} , the radial functions of the strong states are found by numerical integration of coupled and uncoupled radial Schrödinger equations. The strong interaction employed is a Yale hard-core potential¹⁸ with the hard core set at $x_c = \mu_\pi r_c = 0.3375$.

TABLE I. Parameters of the parity-violating internucleon interaction.

Model	A	B	C	C'	D
Conventional	$(-1/\sqrt{2}) \tan\theta^a$	0	0	0	0
Segrè γ_β -invariant	0	0	0	0	$\frac{2}{3}$
Segrè γ_β -noninvariant	-4.0	0	0	$-2/\sqrt{3}$	$\frac{2}{3}$
Lee	$(1/\sqrt{8}) \cot\theta$	1.0	0	$-\sqrt{3}$	0
Extra current	$(1/\sqrt{2}) \cot\theta$	2.0	$-2/\sqrt{3}$	$-2/\sqrt{3}$	$\frac{2}{3}$

^a θ is the Cabibbo angle; we have used $\sin\theta = 0.21$.

¹⁵ References for the various models are given in Ref. 4.

¹⁶ G. Breit and M. L. Rustgi, Phys. Rev. **165**, 1075 (1968).

¹⁷ J. M. Blatt and L. C. Biedenharn, Phys. Rev. **86**, 399 (1952).

¹⁸ The authors are grateful to the Yale N - N phase-shift analysis group for supplying their results prior to publication.

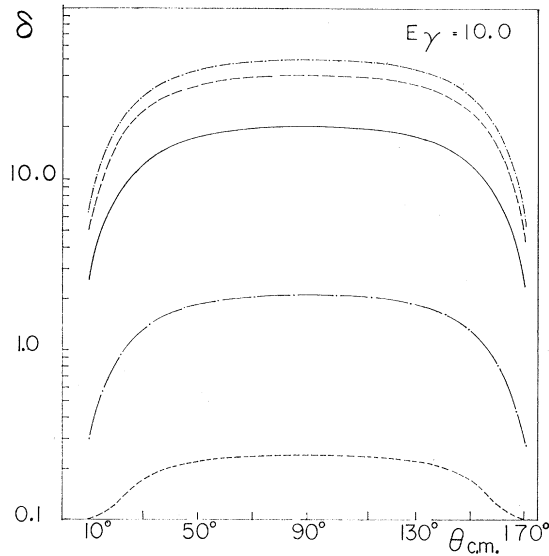


FIG. 1. Absolute value of $\delta \times 10^9$, defined by Eq. (2) for polarized photons of energy $E_\gamma = 10$ MeV. The five curves are for the five models of the weak Hamiltonian: (long dash, dot) conventional; (short dash) Segrè γ_5 -invariant; (medium dash, dot) Segrè γ_5 -noninvariant; (solid line) Lee; (medium dash) extra current.

With this potential and deuteron binding energy equal to 2.22452 MeV, the D -state admixture in the deuteron was calculated to be 5.37%. The weak radial functions were found by converting the differential equations into integral equations and using matrix inversion. The amplitudes for the weak states are, on the average, 10^{-8} smaller from the amplitudes of the strong states.

Reaction amplitudes S_{mm_i} are calculated for photo-

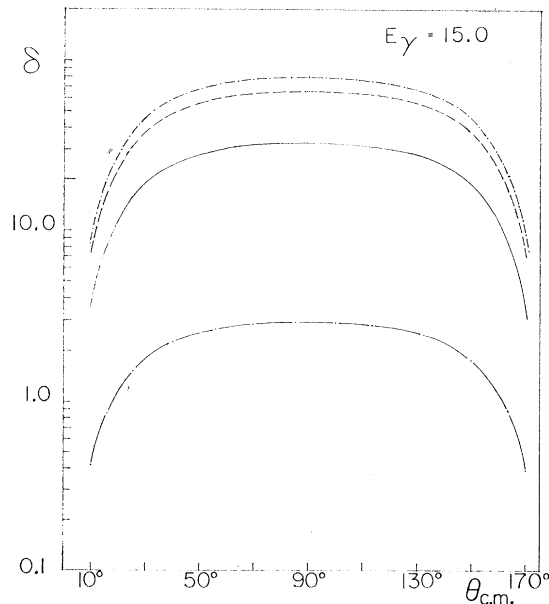


FIG. 2. Absolute value of $\delta \times 10^9$, defined by Eq. (2) for polarized photons of energy $E_\gamma = 15$ MeV. See caption of Fig. 1 for correspondence between curves and models of the weak Hamiltonian.

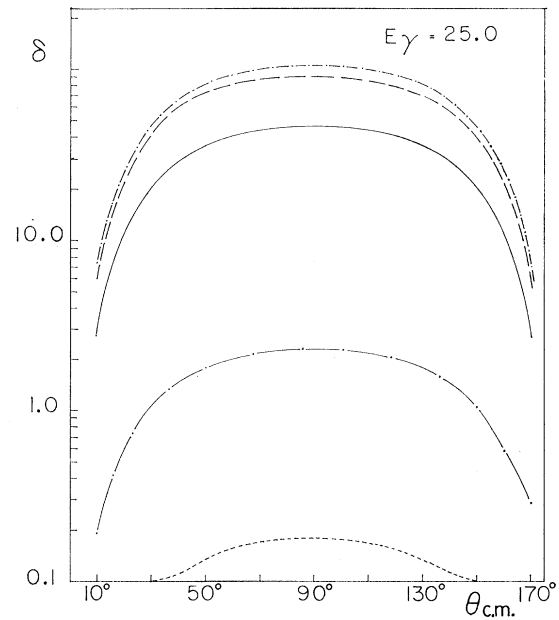


FIG. 3. Absolute value of $\delta \times 10^9$, defined by Eq. (2) for polarized photons of energy $E_\gamma = 25$ MeV. See caption of Fig. 1 for correspondence between curves and models of the weak Hamiltonian.

absorption

$$S_{mm_i} \approx (\psi_m^- | H_{em} | \psi_{m_i}^D)$$

and the Hermitian conjugate of this for photoemission. From S_{mm_i} we calculate functions S_{mi} , from which the cross sections and polarizations are calculated in the manner described in Ref. 14.

The quantities of interest have the following general angular dependence in the $E1-M1$ approximation:

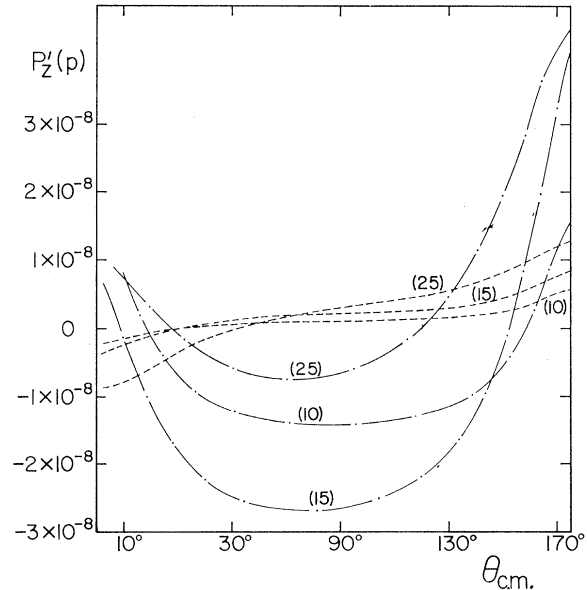


FIG. 4. P_z' component of proton polarization for unpolarized incident photons. The numbers in parentheses indicate energies of incident photons: (long dash, dot) conventional model; (short dash) Segrè γ_5 -invariant model.

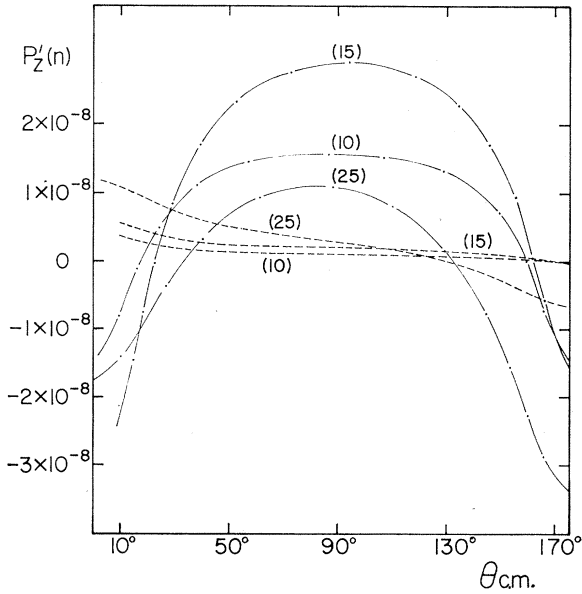


FIG. 5. P_z' component of neutron polarization for unpolarized incident photons. The numbers in parentheses are energies of incident photons: (long dash, dot) conventional model; (short dash) Segrè γ_5 -invariant model.

For deuteron photodisintegration,

$$(a) \quad \delta = \frac{z_4(\theta)}{z_0 + z_1(\theta) + z_2(\theta) \cos^2\phi + z_3(\theta) \sin^2\phi} \sin 2\phi,$$

$$(b) \quad d\sigma P_x' = I(\theta), \quad d\sigma P_z' = J(\theta);$$

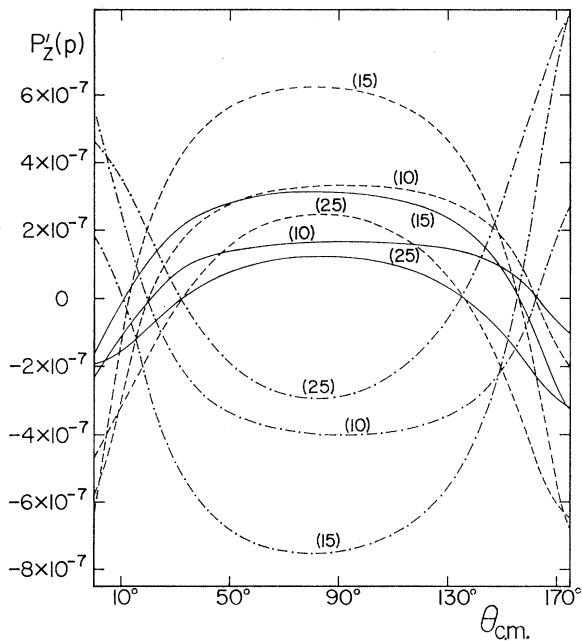


FIG. 6. P_z' component of proton polarization for unpolarized incident photons. The numbers in parentheses are energies of incident photons: (medium dash, dot) Segrè γ_5 -noninvariant; (solid line) Lee; (medium dash) extra current.

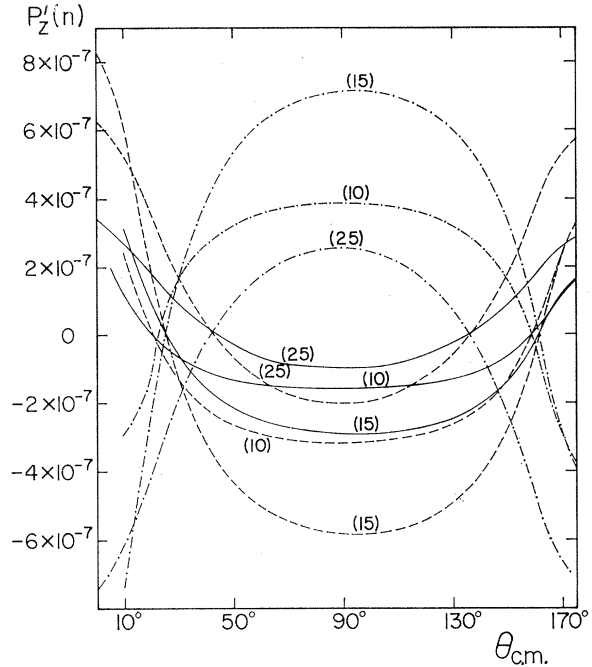


FIG. 7. P_z' component of neutron polarization for unpolarized incident photons. The numbers in parentheses are energies of incident photons: (medium dash, dot) Segrè γ_5 -noninvariant; (solid line) Lee; (medium dash) extra current.

for n - p capture,

$$(c) \quad P_\gamma = L(\theta).$$

Note again that the expressions in (b) are for unpolarized incident photons. The polarization of the emergent neutrons is related to that of the emergent

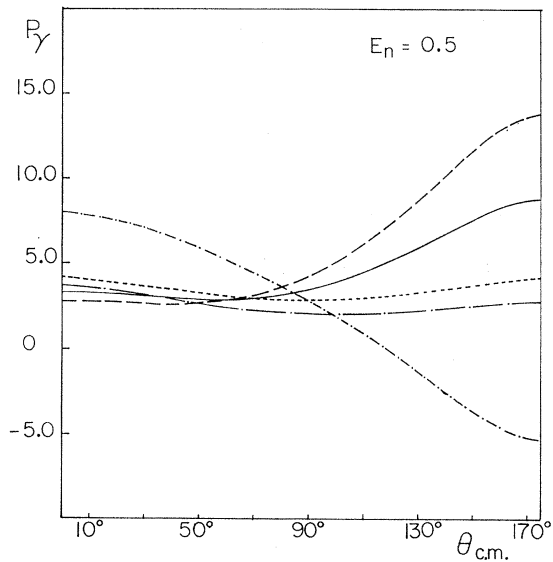


FIG. 8. Circular polarization of photons $P_\gamma \times 10^9$ resulting from n - p capture, for incident neutron energy $E_n = 0.5$ MeV. See caption of Fig. 1 for correspondence between curves and models of the weak Hamiltonian.

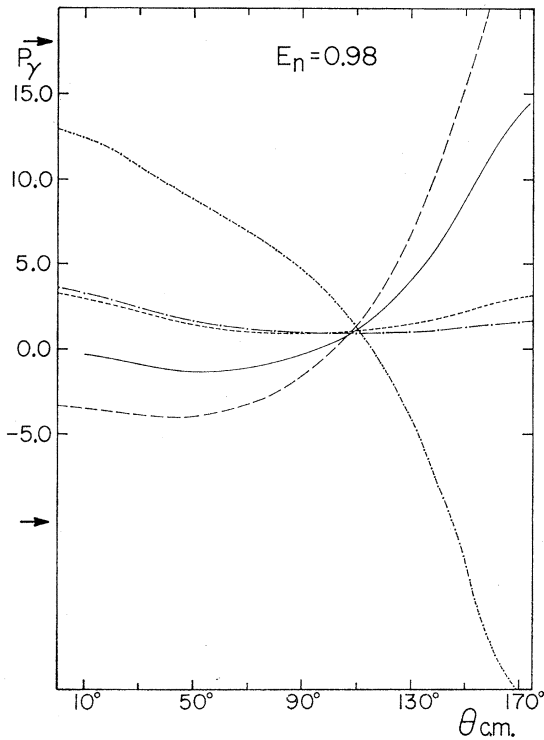


FIG. 9. Circular polarization of photons $P_\gamma \times 10^9$ resulting from n - p capture, for incident neutron energy $E_n = 0.976$ MeV. See caption of Fig. 1 for correspondence between curves and models of the weak Hamiltonian.

protons by the angle transformation $\theta_n = \pi - \theta_p$, $\phi_n = \pi + \phi_p$. In the absence of the weak interaction, $z_4(\theta)$, $I(\theta)$, $J(\theta)$, and $L(\theta)$ vanish.

III. RESULTS AND DISCUSSION

Results of these calculations are shown in Figs. 1–9. Figures 1–3 show the absolute value of the asymmetry $\delta(\theta, \pi/3) \times 10^9$ for three incident-photon energies $E_\gamma = 10$, 15, and 25 MeV. For reasons of economy, we display only the P_z component of proton and neutron polarization for the same three energies, in Figs. 4–7. Finally, Figs. 8 and 9 show the circular polarization $P_\gamma(\theta) \times 10^9$ for two incident-neutron energies $E_n = 0.5$ and 0.976 MeV. We note that the effects of parity violation lie in the range 10^{-9} – 10^{-7} . From the experimental point of view the polarization of protons and neutrons seems more promising than the other parity-violation effects. Our results confirm the estimates of these effects by Blin-Stoyle and Feshbach¹⁰ and the more accurate calculations of Partovi.¹³ On the other hand, the calculations of Tadić⁵ and Danilov¹¹ who, unlike us, used only approximate wave functions for the final and initial state of the nuclear system, show a circular polarization P_γ to be of the order of 10^{-7} in substantial disagreement with our results.

The asymmetry δ in the Segrè γ_5 -invariant model is essentially zero for $E_\gamma = 15$ MeV and hence is not shown

in Fig. 2. For $E_\gamma = 25$ MeV, this δ reappears with negative sign.¹⁹

The large difference, by orders of magnitude, among the effects of parity violation in the five models is due in large measure to the fact which will be discussed below, that the bulk of parity violation comes from the weak pion exchange. Hence the parameter A assumes great importance. We note for example that in the Segrè γ_5 -invariant model with $A = 0$, i.e., no weak pion-exchange interaction, the parity-violation effects are minimal, whereas in the Segrè γ_5 -noninvariant model with $A = -4.0$, the effects are the largest among the five models. Furthermore the large difference in the effects between the conventional model, on one hand, and the Lee and extra-current models, on the other, is due to the fact that in the former model, A is proportional to the tangent of the Cabbibo angle, whereas in the latter, A is proportional to the cotangent of this angle. The contribution of the pion-exchange interaction to the reaction amplitudes is found to be approximately an order of magnitude larger than the contribution of the vector-meson-exchange interaction.²⁰ An indication of the isospin-conserving versus isospin-nonconserving strengths of the weak interaction, the latter being dominated by weak pion exchange, is given in Table II where the percent admixture of the 3P_1 with isospin $T = 1$, and 1P_1 with $T = 0$, in the deuteron, is shown for the five models of the weak Hamiltonian. The percent admixture is defined by

$$\left[\frac{\int_{r_c}^{\infty} Q_i^2 dr}{\int_{r_c}^{\infty} (U^2 + W^2 + Q_I^2 + Q_{II}^2) dr} \right] \times 100,$$

where $i = I$ or II and U , W , Q_I , and Q_{II} are the radial functions for the 3S_1 , 3D_1 , 1P_1 , and 3P_1 states, respectively.

A more direct indication of the relative importance of the weak pion-exchange versus the weak vector-

TABLE II. Percent admixture of 3P_1 and 1P_1 states in the deuteron.

Model	3P_1	1P_1
Conventional ^a	5.5×10^{-15}	8.7×10^{-16}
Segrè γ_5 -invariant ^b	0.0	9.4×10^{-16}
Segrè γ_5 -noninvariant	3.8×10^{-12}	9.4×10^{-16}
Lee	6.5×10^{-13}	1.4×10^{-15}
Extra current	2.6×10^{-12}	2.0×10^{-15}

^a From Table I and Eqs. (6) and (7) one notes that in the conventional model the 3P_1 state is pulled into the deuteron by the pion-exchange weak interaction exclusively, whereas the 1P_1 state arises because of a fraction of the isoscalar part of the vector-meson-exchange interaction.

^b The Segrè γ_5 -invariant model introduces an isoscalar vector-meson-exchange interaction only.

¹⁹ The asymmetry δ is negative in the Lee and extra-current models for $E_\gamma = 10$, 15, and 25 MeV, negative in the Segrè γ_5 -invariant model for $E_\gamma = 25$ MeV and positive in all other cases.

²⁰ This effect depends strongly on the short-range correlations introduced by the strong nucleon-nucleon interaction. In the present case, the hard core at $x = \mu_{\pi r} = 0.3375$ is substantially responsible for the smaller contribution of the weak vector-meson exchange interaction; see J. Barclay Adams, Phys. Letters 22, 463 (1966).

meson-exchange contribution to the parity-violating interaction is shown in Figs. 10 and 11 where δ and P_z' are plotted, in the conventional model, first with parameters $A, B, C, C',$ and D as shown in Table I and then with the weak vector-meson-exchange contribution completely switched off. The incident photon energy is 10 MeV. We note that, on the average, the difference between including and excluding the vector-meson-exchange interaction is 10% for δ and 8% for the polarization.

Finally the sensitivity of the effects on the range of the vector-meson-exchange interaction was checked by reducing arbitrarily the ρ -meson mass from 765 MeV to 745 MeV, i.e., by almost 3%. As expected, the change in the magnitude of the parity-violating effects was different for different models of H_w , depending on the strength of the dominating weak pion exchange. For example, in the Segrè γ_5 -invariant model which has no contribution from weak pion exchange, the effects were increased by almost 11%, whereas in the Segrè γ_5 -noninvariant model with parameter $A = -4.0$, the change in the effects of parity violation was less than 1%.

One more comment is in order. The statement made by Tadić⁵ that only the isoscalar part of the weak interaction contributes to the circular polarization P_γ , is true provided that n - p capture is taking place from an initial ${}^1S_0(T=1)$ state only, and provided the $E1$ effect is calculated by the usual $-e(\mathbf{E} \cdot \mathbf{r})$ form. The argument is very simple. P_γ is proportional to $M1$

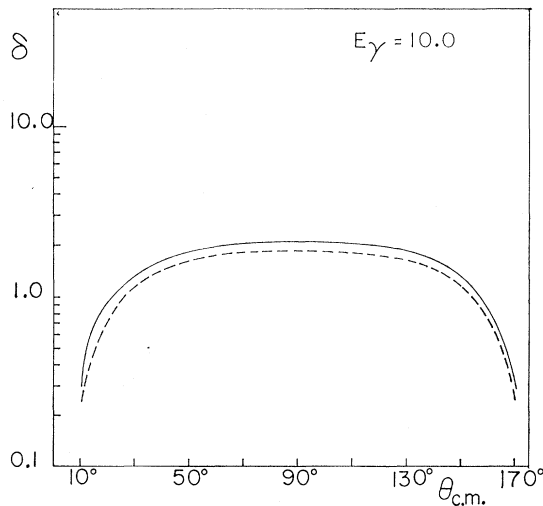


FIG. 10. Absolute value of $\delta \times 10^9$ defined by Eq. (2) for polarized photons of energy $E_\gamma = 10$ MeV in the conventional model with pion exchange and vector-meson exchange (solid line), and with pion exchange only (medium dash).

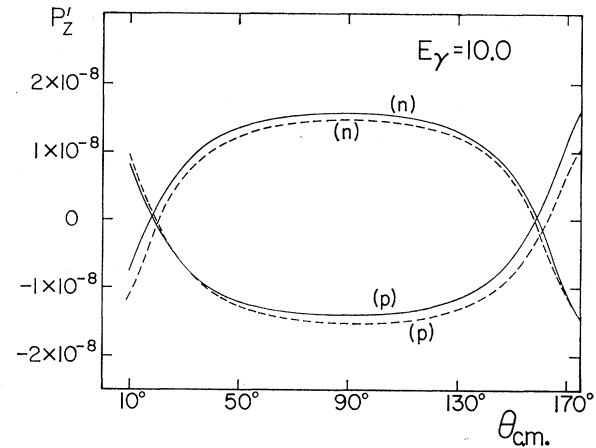


FIG. 11. P_z' component of proton (p) and neutron (n) polarization for incident unpolarized photons of energy $E_\gamma = 10$ MeV in the conventional model with pion exchange and vector-meson exchange (solid line), and with pion exchange only (medium dash).

$\times E1$.¹⁰ The only possible $E1$ transition from ${}^1S_0(T=1)$ is to the deuteron ${}^1P_1(T=0)$ state which, in turn, is admixed into the deuteron by the isoscalar part of the weak potential. If, on the other hand, partial waves other than 1S_0 are available in the initial state, then the entire weak potential may contribute to P_γ . We have checked these facts by calculating P_γ for incident-neutron energy very close to zero. With the isoscalar part of the vector-meson-exchange interaction V_1^V turned off, P_γ was reduced essentially to zero. When V_1^V was turned on, in the conventional model we obtained $P_\gamma = 3.1 \times 10^{-9}$, fairly constant over the angular range $0^\circ \leq \theta_{c.m.} \leq 180^\circ$.

In conclusion, we find that the effects of parity violation are substantially different for different models of the weak Hamiltonian, so that when experimental measurements become available, one should be able to discriminate among the existing models.

ACKNOWLEDGMENTS

One of us (E. H.) wishes to express his deep appreciation for the encouragement, interest in this work, and hospitality extended to him by Professor G. E. Brown at the State University of New York at Stony Brook where most of this work was done. Thanks are also due to Dr. G. Scharff-Goldhaber for useful discussions and for making available to us excellent computing facilities at Brookhaven National Laboratories. We also wish to express our indebtedness to Professor D. Tadić for his interest in the early stages of this calculation.